



Cite this: *Chem. Sci.*, 2021, **12**, 3328

All publication charges for this article have been paid for by the Royal Society of Chemistry

Phenazines as model low-midpoint potential electron shuttles for photosynthetic bioelectrochemical systems†

Eleanor R. Clifford,‡^a Robert W. Bradley, ID,‡^b Laura T. Wey, ^c Joshua M. Lawrence, ^c Xiaolong Chen, ^a Christopher J. Howe ID, *^c and Jenny Z. Zhang ID, *^a

Bioelectrochemical approaches for energy conversion rely on efficient wiring of natural electron transport chains to electrodes. However, state-of-the-art exogenous electron mediators give rise to significant energy losses and, in the case of living systems, long-term cytotoxicity. Here, we explored new selection criteria for exogenous electron mediation by examining phenazines as novel low-midpoint potential molecules for wiring the photosynthetic electron transport chain of the cyanobacterium *Synechocystis* sp. PCC 6803 to electrodes. We identified pyocyanin (PYO) as an effective cell-permeable phenazine that can harvest electrons from highly reducing points of photosynthesis. PYO-mediated photocurrents were observed to be 4-fold higher than mediator-free systems with an energetic gain of 200 mV compared to the common high-midpoint potential mediator 2,6-dichloro-1,4-benzoquinone (DCBQ). The low-midpoint potential of PYO led to O₂ reduction side-reactions, which competed significantly against photocurrent generation; the tuning of mediator concentration was important for outcompeting the side-reactions whilst avoiding acute cytotoxicity. DCBQ-mediated photocurrents were generally much higher but also decayed rapidly and were non-recoverable with fresh mediator addition. This suggests that the cells can acquire DCBQ-resistance over time. In contrast, PYO gave rise to steadier current enhancement despite the co-generation of undesirable reactive oxygen species, and PYO-exposed cells did not develop acquired resistance. Moreover, we demonstrated that the cyanobacteria can be genetically engineered to produce PYO endogenously to improve long-term prospects. Overall, this study established that energetic gains can be achieved via the use of low-potential phenazines in photosynthetic bioelectrochemical systems, and quantifies the factors and trade-offs that determine efficacious mediation in living bioelectrochemical systems.

Received 13th October 2020
Accepted 14th January 2021

DOI: 10.1039/d0sc05655c
rsc.li/chemical-science

Introduction

Oxygenic photosynthetic microorganisms can be 'wired' (electrically connected) to electrodes to harness light energy for electrical power generation in biophotovoltaic (BPV) systems (Fig. 1A),^{1–4} and potentially for fuel generation in semi-artificial photosynthesis.⁵ Cyanobacteria are particularly attractive biocatalysts for these biotechnologies since they are abundant, simple in cellular architecture, can reproduce and self-repair, have wide-ranging biosynthetic capabilities, and contain

efficient photo-harvesting machineries for carrying out endergonic reactions.^{1,6,7} However, although photosynthetic microorganisms are known to give rise to steady and long-lived photocurrents,⁸ the output magnitudes are also much lower compared to isolated proteins and synthetic systems.^{5,9} Artificially added exogenous electron mediators are therefore widely used for efficient wiring of the photosynthetic cells to electrodes.

Benzoquinones are common electron mediators found in electron transport chains and synthetic derivatives are commonly used as exogenous electron mediators.^{8,10} A typical benzoquinone used as the exogenous mediator for both protein and cell-based photoelectrochemical systems is 2,6-dichloro-1,4-benzoquinone (DCBQ, midpoint potential: $E_m = 0.315$ V vs. SHE¹¹).^{5,12} During photosynthesis, electrons derived from water oxidation at photosystem II (PSII) are fed into the photosynthetic electron transport chain (PETC) in the thylakoid membranes.^{8,13} In the absence of exogenous mediators, some electrons leave the PETC downstream of photosystem I (PSI) to participate in extracellular electron transfer, which then give

^aDepartment of Chemistry, University of Cambridge, Lensfield Road, Cambridge CB2 1EW, UK. E-mail: jz366@cam.ac.uk

^bDepartment of Life Sciences, Sir Alexander Fleming Building, Imperial College, SW7 2AZ, UK

^cDepartment of Biochemistry, University of Cambridge, Tennis Court Road, Cambridge, CB2 1QW, UK. E-mail: ch26@cam.ac.uk

† Electronic supplementary information (ESI) available. See DOI: [10.1039/d0sc05655c](https://doi.org/10.1039/d0sc05655c)

‡ These authors contributed equally to the paper.



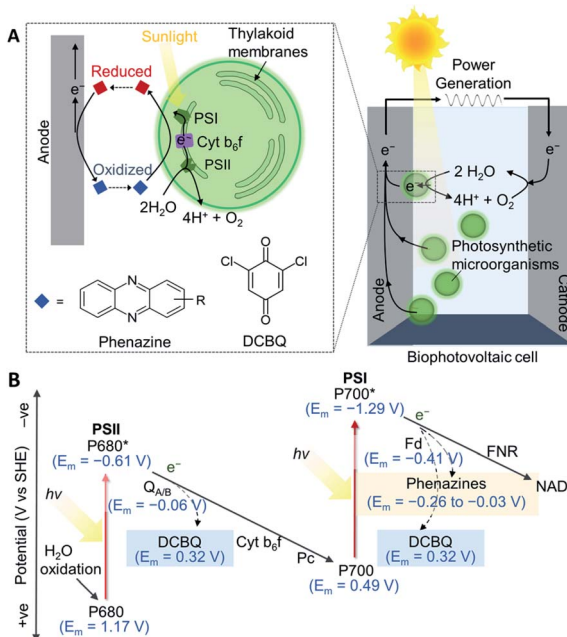


Fig. 1 (A) A schematic of a biophotovoltaic (BPV) system employing photosynthetic microorganisms at the anode. Under illumination, photosynthetic microorganisms oxidize H_2O to O_2 and H^+ and transfer some of the resulting energized electrons to an anode. The electrons flow to the cathode, where O_2 is catalytically reduced to reform H_2O , generating a current. At the anode, an indirect extracellular electron transfer (EET) pathway is shown, where electron transfer is mediated by a redox molecule diffusing between the intracellular electron donors and the electrode surface. (B) Energetic landscape of the photosynthetic electron transport chain (PETC; shown by solid arrows): electrons are derived from H_2O oxidation by photosystem II (PSII), photoexcited by the reaction center, P680,^{16,17} and exit via the terminal quinones, $Q_{A/B}$. The plastoquinone pool passes electrons to the cytochrome b_6f complex (Cyt b_6f), which shuttles electrons via plastocyanin (P_c) to photosystem I (PSI).¹⁸ The electrons are picked up by ferredoxin (Fd), and delivered to ferredoxin-NADP⁺ reductase (FNR)¹⁹ to reduce NADP⁺. The dashed arrows represent the points from which electrons can be intercepted by 2,6-dichloro-1,4-benzoquinone (DCBQ)¹¹ and phenazines.^{20,21} All midpoint potentials (E_m) correspond to pH 7.

rise to photocurrents if the electrons are collected by an electrode (Fig. 1).¹⁴ DCBQ is hypothesized to function similarly to the terminal photosystem II (PSII) electron acceptor, Q_B , and extract electrons from the PETC downstream of PSII.^{8,10} However, exogenous electron mediators such as DCBQ have poorly defined modes of toxicity, and have high scale-up costs.^{8,10,15} Also, the positive E_m value of DCBQ means that mediation comes with a significant thermodynamic cost (Fig. 1B),¹¹ where the potential difference between the terminal acceptor for PSI and DCBQ is approximately 700 mV. The identification of efficacious electron mediators capable of enhancing photocurrents at potentials more negative than mediators like DCBQ would allow more energy to be recovered from photosynthesis and be a breakthrough in the field. Further gains could be made by producing electron mediators endogenously. However, design principles for effective endogenous or exogenous mediators are currently lacking.

Phenazines are a class of redox-active secondary metabolites produced by a few clades of bacteria, most notably pseudomonads,^{20,22} but not cyanobacteria.²³ They have been shown to enhance current outputs from microbial fuel cells (MFCs)^{24–28} but have not yet been explored as mediators for cyanobacteria or BPVs. Phenazines are suitable electron shuttles since they are small and lipid-soluble^{6,21} and are therefore able to pass through bacterial membranes to facilitate EET. They have E_m values more negative than DCBQ, but still positive enough to accept electrons from the PETC (Fig. 1B).^{11,18–21,29} Additionally, they have considerable bioengineering potential as the genetics and biochemistry of their biosynthesis are well understood,^{20,23} though cyanobacteria have not been engineered for their biosynthesis.

Here, we assessed an approach for improving indirect mediation for cyanobacteria—using lower midpoint potential electron mediators to minimise energy loss, with phenazines as the model mediators. A library of phenazines was tested as electron mediators for *Synechocystis* sp. PCC 6803 (hereafter *Synechocystis*), which is a model cyanobacterium for BPVs. We identified pyocyanin (PYO) as a promising low-potential candidate and tested the limits of its mediation ability in terms of energetics, permeability, concentration required for mediation, cytotoxicity, overall longevity and potential for endogenous production in cyanobacteria. We revealed benefits and limitations of both phenazines and benzoquinones relating to their modes of mediation and deactivation.

Results and discussion

Phenazine screening

Four phenazines (Fig. 2A) were initially screened as potential electron mediators for BPVs: phenazine (PHZ), 1-hydroxyphenazine (1-OHP), phenazine-1-carboxylic acid (PCA) and PYO. 1-OHP, PCA and PYO were of interest as they can be endogenously synthesized by bacteria such as *Pseudomonas aeruginosa*,^{2,6} and can potentially be introduced endogenously into microbial electrochemical systems either by genetic modification or through a co-culturing approach.³⁰ PHZ contains the basic phenazine backbone and was included as a control.

Suitable electron mediators for photosynthetic organisms should exhibit E_m values more positive than key components of the PETC (>-0.41 V vs. SHE, Fig. 1B) to favour kinetics of electron transfer; however, those with very positive E_m values will result in significant energy losses. The E_m value of each mediator candidate was measured using cyclic voltammetry under typical BPV conditions (in BG11 medium at pH 8.5 in which the cyanobacterial cultures were grown to favour bicarbonate uptake into the cells, Fig. S1†). All candidates showed a single anodic and cathodic peak corresponding to a concerted two-proton two-electron oxidation and reduction, respectively.^{31,32} The redox reactions of all mediator candidates considered in this study are shown in Fig. S3.† The E_m values of the phenazines fell within the range -0.120 to -0.252 V vs. SHE, whereas DCBQ exhibited a more positive E_m value of 0.250 V vs. SHE. As the redox reactions of phenazines and benzoquinones are



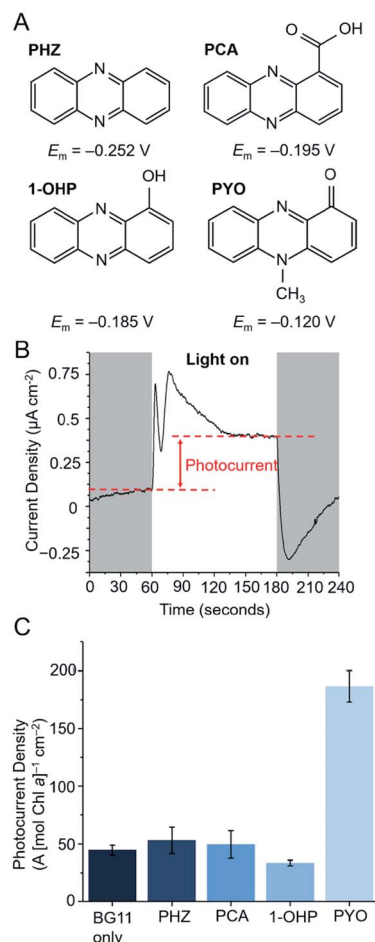


Fig. 2 Photoelectrochemical screening of phenazines for their ability to mediate electrons between *Synechocystis* and an electrode. (A) Structures and midpoint potentials (E_m) of the phenazines screened. The E_m potentials of the phenazines were measured in BG11 media at pH 8.5 and are reported vs. SHE. (B) A typical chronoamperometry profile obtained of a *Synechocystis*-loaded ITO electrode under dark/light cycles at an applied potential of 0.3 V vs. SHE; the photocurrent is defined by the difference between the steady-state dark and light currents. (C) Chl a normalised photocurrent densities of *Synechocystis*-loaded electrode in the presence of four different phenazines (200 μ M). All chronoamperometry measurements were recorded at an applied potential of 0.3 V vs. SHE, and under atmospheric conditions at 25 °C in BG11 medium electrolyte. Light conditions used: $\lambda = 680$ nm, 1 mW cm $^{-2}$ (50 μ E m $^{-2}$ s $^{-1}$). The mean was taken from three biological replicates and the error bars represent the standard error of the mean ($n = 3$).

proton coupled,^{31,32} their electrochemical properties are pH dependent and the E_m values observed for pH 8.5 were negatively shifted (by *ca.* 90 mV) compared to experimental and reported values obtained near pH 7 (Fig. S2†).^{20,21,33}

Thermodynamically, all four phenazines can accept electrons downstream of PSI. The P680 and P700 reaction centers presumably cannot directly reduce the phenazines as they are embedded deep within protein complexes and are difficult for mediators to access.^{34,35} The more positive E_m value of PYO suggests that it could also be reduced to a small extent by the terminal quinones (Q_B $E_m = -0.06$ V vs. SHE²⁹). This is not

expected for the other phenazines as their E_m values are more negative than that of $Q_{A/B}$. DCBQ is a commonly used electron mediator that targets PSII,^{8,10} but its positive E_m value suggests that it can also accept electrons from PSI. To test the ability of the phenazines to mediate electron transfer in microbial photoelectrochemical systems, a previously described three-electrode photoelectrochemical set-up using the model cyanobacterium *Synechocystis* was employed (Fig. 2A).⁸ *Synechocystis* cells were first dropeast as a concentrated planktonic culture (150 nmol Chl a mL $^{-1}$) onto a porous inverse opal indium tin-oxide (IO-ITO) electrode, allowing cell adsorption over 16 h in the dark. The Chl a loading was determined afterwards, with average Chl a loading 3.26 μ g Chl a cm $^{-2}$ (5 nmol Chl a per electrode).

In a typical chronoamperometry experiment, illumination of the *Synechocystis*-loaded working electrode induces a photocurrent corresponding to a change in electron flux from the photosynthetic microorganism to the electrode (Fig. 2B). A diffusional mediator serves to enhance the photocurrent by increasing the flux of electrons from the microorganism to the electrode, but this will only take place when the electrode is at a potential that can oxidize the mediator and when the mediator is above a threshold concentration. Chronoamperometry experiments using a bare IO-ITO electrode confirmed that the observed photocurrents stemmed from the photosynthetic microorganisms (Fig. S4†).

Previous studies by Grattieri *et al.* have shown that measuring the E_m of quinone redox mediators in aqueous environments is not sufficient when trying to understand their ability to mediate EET in photosynthetic purple bacteria.³⁶ This is due to contributions by the lipophilic membranes that the mediators must traverse, and also the E_m corresponds to a 2e $^-$ /2H $^+$ process that does not often accurately reflect the electron exchange processes occurring within biological contexts. The E_m values discussed should therefore be treated only as a helpful guide for comparing thermodynamics between redox species. To determine the minimum applied potential needed for photocurrent enhancement by a phenazine electron mediator, PYO was introduced to the photoelectrochemical cell and stepped chronoamperometry experiments were performed (Fig. S5†). Competing charge transfer pathways in the form of photocathodic currents have been known to obfuscate the photocurrents at potentials <0.2 V vs. SHE. These are due to the reduction of oxygen (onset at 0 V vs. SHE, Fig. S4C†) or reactive oxygen species (ROS) at the electrode.^{29,37} Maximum photocurrents were observed at 0.3 V vs. SHE, which is 0.2 V more negative than the applied potential required to observe the maximum photocurrent mediated by DCBQ (0.5 V vs. SHE).¹¹ Since the other phenazines have more negative E_m values than PYO, their onset potentials are expected to convey the same trend, and subsequent chronoamperometry experiments involving phenazines were carried out with an applied potential of 0.3 V vs. SHE.

The photocurrent densities from *Synechocystis*-loaded electrodes in the presence of 200 μ M of each of the phenazines at 0.3 V vs. SHE are shown in Fig. 2C. To take account of possible cytotoxicity effects and other sources of variation in cell

numbers, the Chl *a* content of each electrode was quantified after each experiment and the photocurrent densities presented are normalised by Chl *a* content on the electrode. PYO gave rise to a 4-fold enhancement in photocurrent density; the other phenazines did not exhibit mediation. To understand whether the lack of mediation by the other phenazines may be attributed to poor cell permeability, clog *D* values were calculated at a range of pH values for each phenazine. clog *D* values are computationally determined partition coefficients, which have been developed to predict the permeability of drugs through mammalian plasma membranes.³⁸ A clog *D* value of greater than 0.5 is required for a 50% probability of the molecule being highly permeable to cell membranes.³⁸ Using this predictor, the oxidised and reduced states of PHZ, 1-OHP and PYO are expected to permeate into the cell due to their high clog *D* values at the media pH of 8.5, as well as out of the cell due to their high clog *D* values at the cytoplasmic pH of 7.5 (Fig. S6†). In contrast, PCA was predicted to be membrane impermeable in both its oxidised and reduced states and therefore unable to perform mediation. All phenazines had a sufficiently high clog *D* value at the thylakoid lumen pH of 4.6, suggesting mediators are not sequestered within this compartment. The poor mediation ability of PHZ and 1-OHP, despite their predicted membrane permeability, may be attributed to factors such as poor aqueous solubility or low driving force for electron transfer. PYO, having been found to be the most promising mediator from the screening, was taken forward and compared with the model benzoquinone mediator, DCBQ.

Cytotoxicity versus mediation concentration

The efficacy of a diffusional mediator depends on it being in excess at the bio-electrode interface. For efficient shuttling, bulk concentrations of $>100\ \mu\text{M}$ are typically employed.^{8,10,14,39–41} However, an often-neglected trade-off is the toxicity of the mediator towards the living cells, which also scales with the concentration of the mediator present. Although DCBQ cytotoxicity is often observed^{8,10} and a non-photochemical quenching effect of DCBQ has been described,⁴² the effect of DCBQ concentration on the growth of photosynthetic microorganisms has not been tested to the best of the authors' knowledge.

Spot assays were performed to probe the effect of different concentrations of PCA, PYO and DCBQ on *Synechocystis* growth to identify the highest concentration of mediator at which the cells could still grow (Fig. 3A) and the time course over which this concentration was non-toxic (Fig. 3B). PCA was included because it is the precursor from which PYO is derived,^{23,43} so is likely to be present in anticipated PYO-producing cells.

Equivalent amounts of *Synechocystis* cells to those that adhered to the IO-ITO electrodes for photoelectrochemical tests (5 nmol Chl *a*) were incubated with PCA, PYO, and DCBQ at different concentrations for 1 or 3 days under constant light ($1\ \text{mW}\ \text{m}^{-2}$ ($50\ \mu\text{E}\ \text{m}^{-2}\ \text{s}^{-1}$))). Concentration ranges of up to 0.5 mM were tested for PCA and PYO due to their limited aqueous solubility. It was possible to test concentration ranges of up to 1 mM for DCBQ, and this was done to parallel previous photoelectrochemical experiments.^{8,33}

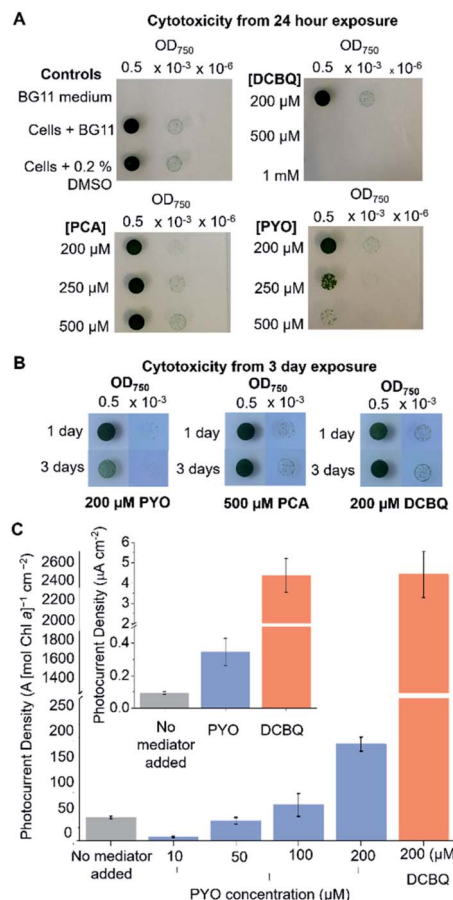


Fig. 3 Mediator concentrations giving rise to cytotoxicity and photocurrent enhancement. (A) Cytotoxicity spot assay to determine the effect of PYO, PCA and DCBQ on the growth of *Synechocystis*. *Synechocystis* cells (5 nmol Chl *a*) were incubated with the mediators at different concentrations for 24 h under $1\ \text{mW}\ \text{m}^{-2}$ ($50\ \mu\text{E}\ \text{m}^{-2}\ \text{s}^{-1}$) white light. The cells were resuspended in BG11 and their concentration standardized to an OD₇₅₀ of 0.5. Serial dilutions were prepared, spotted on agar and incubated for 1 week. Data from a single representative plate from 3 replicates is shown. (B) The spot assay was repeated for the highest concentration of mediators that did not inhibit cell growth after 24 h, with the incubation period extended to 3 days. (C) Chl *a* normalised initial photocurrent densities from *Synechocystis* in the presence of different concentrations of PYO and DCBQ (200 μM). Inset: initial photocurrent densities from *Synechocystis* in the presence of PYO (200 μM) and DCBQ (200 μM), without normalization by Chl *a* content. All chronoamperometry measurements were recorded at an applied potential of 0.3 V vs. SHE, except for measurements made using DCBQ, which were performed at an applied potential of 0.5 V vs. SHE under atmospheric conditions at $25\ ^\circ\text{C}$ in BG11 medium. Light conditions used: $1\ \text{mW}\ \text{cm}^{-2}$ ($50\ \mu\text{E}\ \text{m}^{-2}\ \text{s}^{-1}$) of 680 nm wavelength. The mean was taken from three biological replicates and the error bars represent the standard error of the mean ($n = 3$).

After exposure to the mediators, the *Synechocystis* cells were re-suspended in fresh BG11 medium, spotted onto BG11 agar plates, and incubated for 1 week. Three control conditions were also assayed: BG11 only (no cells), cells in BG11 (no mediator), and cells in BG11 with 0.2% (v/v) DMSO (the highest concentration of DMSO solvent in the DCBQ cytotoxicity tests) as



shown in Fig. 3A and S7.† The quantity of DMSO employed was confirmed to be non-toxic.

As shown in Fig. 3A, *Synechocystis* incubated for 1 day with 200 μ M PYO or 200 μ M DCBQ showed growth comparable to the controls, indicating that exogenously added PYO and DCBQ were non-toxic at concentrations <200 μ M. At higher concentrations of mediator, the cells showed significantly poorer growth than the controls, indicating cytotoxicity at concentrations >200 μ M. Cells incubated with PCA showed comparable growth to the controls, indicating that exogenously added PCA is non-toxic to at least 500 μ M even after 3 days of incubation; this is consistent with its predicted low cell membrane permeability (Fig. S6†).

Synechocystis cells incubated for 3 days with 500 μ M PCA or 200 μ M DCBQ showed growth comparable to the controls (Fig. 3B and S7†), indicating that exogenously added PCA and DCBQ at these concentrations are non-toxic for 3 days. Cells incubated for 3 days with 200 μ M PYO exhibited noticeably poorer growth than the controls, indicating that exogenously added PYO at higher concentrations is toxic in the long-term. This may be attributed to the ability of PYO to produce harmful ROS upon interaction with oxygen.^{20,44–47}

To ascertain the minimum concentration of PYO needed for efficient electron shuttling, chronoamperometry with dark/light cycles using *Synechocystis*-loaded IO-ITO electrodes was performed in the presence of different concentrations of PYO. Based on the results of the cytotoxicity assay, 200 μ M was chosen as the maximum concentration of PYO to be tested. Interestingly, when incubated with 10 μ M PYO, the photocurrent diminished to less than 50% of the no-mediator condition (Fig. 3C); however, photocurrent enhancement was observed at concentrations >100 μ M. A likely explanation for the different mediation behaviour of PYO with concentration change is that PYO (-0.120 V vs. SHE, pH 8.5) may inhibit EET analogous to methyl viologen ($E_m = -0.42$ V vs. SHE¹⁴), which can intercept electrons from PSI in the PETC and reduce O_2 .^{48,49} We hypothesize that after PYO is reduced, O_2 is in competition with the electrode to accept electrons from reduced PYO. At concentrations of PYO <200 μ M under atmospheric conditions, O_2 (present at around 250 μ M in aqueous solution) can intercept most electrons before PYO can shuttle them to the electrode, reducing the photocurrent observed. At higher concentrations of PYO, more reduced mediator can reach the electrode, giving rise to the photocurrent enhancement. To test this, the chronoamperometry experiments were repeated in 10 μ M PYO with N_2 bubbling to purge O_2 from the electrolyte, though it is difficult to remove O_2 completely from an oxygenic photosynthetic system. Decreasing the O_2 concentration in the electrolyte restored the photocurrent to approximately 80% of that obtained in the absence of mediator (Fig. S8†), indicating that O_2 was competing with the electrode to accept electrons from reduced PYO.

It can be concluded that for PYO to serve as an efficient electron mediator for *Synechocystis*, a concentration of between 100–200 μ M should be used to enhance photocurrents whilst still minimizing acute cytotoxicity. It was previously demonstrated that this concentration range of PYO can be

endogenously expressed by *Pseudomonas aeruginosa*,⁵⁰ hence the concentration needed for mediation in BPVs may be feasibly achieved with bio-engineering and/or a co-culturing approach.

The initial photocurrents of *Synechocystis*-loaded IO-ITO electrodes mediated by 200 μ M PYO or DCBQ were compared (Fig. 3C inset). *Synechocystis*-loaded electrodes in the presence of PYO and DCBQ produced ca. 4-fold and 40-fold greater initial photocurrent densities, respectively, compared to electrodes with no exogenous mediator. It should be noted that the initial photocurrents reported here for DCBQ are an order of magnitude lower than those reported when higher, cytotoxic, concentrations of DCBQ were used.⁸ Hence, PYO harvested

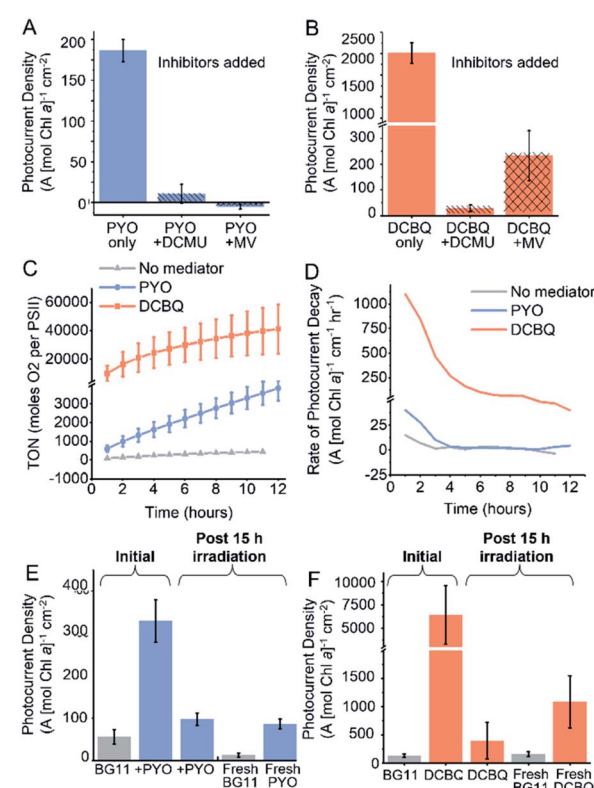


Fig. 4 Mediation mechanism and longevity. Chl a normalized initial photocurrent densities from *Synechocystis* in the presence of (A) PYO (200 μ M) and (B) DCBQ (200 μ M) and the PETC inhibitors 3-(3,4-dichlorophenyl)-1,1-dimethylurea (DCMU, 1 mM) or methyl viologen (MV, 1 mM). (C) Turn-over numbers (TON) of *Synechocystis*-loaded IO-ITO electrodes per PSII in the presence of PYO (200 μ M) and DCBQ (200 μ M) over 15 h of light exposure. (D) Rates of photocurrent decay of *Synechocystis*-loaded IO-ITO electrodes in the presence of PYO (200 μ M) and DCBQ (200 μ M) over 15 h of light exposure. (E and F) Photocurrent densities from *Synechocystis*: without the addition of mediators (BG11), after addition of 200 μ M PYO (+PYO) and DCBQ (+DCBQ) and after 15 h light exposure with the mediator, after replacement with fresh BG11 media (fresh BG11), and after the addition of 200 μ M fresh PYO (fresh PYO) or DCBQ (fresh DCBQ). All chronoamperometry measurements were recorded at an applied potential of 0.3 V vs. SHE under atmospheric conditions at 25 °C in BG11 medium electrolyte, except for measurements made with DCBQ, which were performed at 0.5 V vs. SHE. Light conditions used: 1 mW cm^{-2} (50 μ E m^{-2} s^{-1}) of 680 nm chopped light. The mean was taken from three biological replicates and the error bars represent the standard error of the mean ($n = 3$).



a significantly smaller fraction of the cells' available reducing equivalents compared to DCBQ. There are several likely explanations for this. Firstly, PYO and DCBQ have different intracellular targets and the positive E_m value of DCBQ means that it could be reduced by more components of the PETC. Additionally, the more positive E_m value of DCBQ imparts it with a greater thermodynamic driving force for reduction, which also increases the electron transfer kinetics. Lastly, reduced PYO has a competing O_2 reduction side-reaction, which does not occur for DCBQ due to its higher E_m value.

Sites of mediator reduction

To probe the site of reduction of PYO and DCBQ within the PETC, two PETC inhibitors were used in chronoamperometry experiments: 3-(3,4-dichlorophenyl)-1,1-dimethylurea (DCMU) and methyl viologen (Fig. 4A). DCMU inhibits electron flow downstream of PSII by competing with Q_B^{29} and preventing electron transfer from PSII to the plastoquinone pool (Fig. 4B).¹⁴ As previously described, methyl viologen competes for electrons downstream of PSI and transfers them to O_2 .¹⁴ Combining PYO with methyl viologen completely ablated the photocurrents originating from *Synechocystis*, consistent with PYO accepting electrons downstream of PSI. Findings from a previous study suggested that phenazines can compete with NAD^+ for reduction by enzymes within the cell; in the photosynthetic context PYO may be able to accept electrons from the ferredoxin:NADP⁺ reductase.⁵¹ The addition of DCMU to PYO mediated systems almost completely eliminated any mediation effects (11 A [mol Chl a]⁻¹ cm⁻²). Small photocurrents (28 A [mol Chl a]⁻¹ cm⁻²) were still observed when DCMU was added to DCBQ mediated systems. This indicates that although water oxidation has been inhibited by the DCMU, electron flow downstream of PSII can still contribute towards EET. It is possible that some electron flow continues in the presence of DCMU because the respiratory and photosynthetic electron transfer chains in *Synechocystis* share the same plastoquinone pool.¹⁴ Combining DCBQ with methyl viologen resulted in a 10-fold decrease in the photocurrent yielded by DCBQ mediation, but this photocurrent was still 4-fold greater than the no-mediator condition (Fig. 2C). This is consistent with DCBQ being able to accept electrons upstream of PSI even though electrons downstream of PSI are intercepted by MV. The observation that the presence of methyl viologen could significantly diminish the photocurrent mediated by DCBQ suggests that EET can stem from downstream of PSI. These results confirm that PYO and DCBQ have different intracellular targets and mechanisms of EET mediation.

Mediator longevity

It is well documented that the electron mediation effects of DCBQ drop off quickly over time and the decrease in effectiveness is accompanied by a poorly characterized non-photochemical quenching effect.^{8,42} To study the longevity of the mediation by both PYO and DCBQ, chronoamperometry was carried out over 15 h under constant illumination. In the absence of exogenous mediators, the photocurrent was observed to remain constant for over 15 h, consistent with

photocurrents previously observed for living cells.⁸ In cases where mediators were introduced, immediately following mediator addition, a sharp rise in photocurrent could be observed, which decayed rapidly to a steady rate at *ca.* 80 min (Fig. S9†). The rapid initial decay in photocurrent could be attributed to the time needed for the electrode double layer to reach equilibrium and the decay in the concentration of reduced mediator species at the electrode surface over time, since the system was unstirred and mass transport was likely to be a limitation.

The turn-over number (TON), which is proportional to the cumulative charge collected by the *Synechocystis*-loaded electrodes over 12 h is summarized in Fig. 4C and S9.† The turn-over frequency (TOF) relating to the rate of oxygen evolution per PSII was generated based on the assumption that the ratio of PSI : PSII was 1 : 1 in the PETC, and that the faradaic efficiency for oxygen evolution in relation to the photocurrent output is near unity (Fig. S9B†).

DCBQ was observed to give rise to greater than 10-fold higher TON and TOF numbers compared to PYO, but the rate of decay in the mediated photocurrent also vastly exceeded that of PYO. After the initial drop in photocurrent, the DCBQ mediated system continued to decay at *ca.* 100 A (mol Chl a)⁻¹ cm⁻¹ h⁻¹ after 6 h, whereas the PYO mediated system showed near-zero decay rates after 3 h (Fig. 4D). This implies that PYO mediation has a different deactivation mechanism from DCBQ, which has been reported to exert quenching of the photoexcited Chl a within the PETC upon close interactions.^{42,52,53} After 15 h, the DCBQ mediated photocurrent decreased 12-fold (Fig. 4); in contrast, the PYO-mediated system decreased 3-fold. In the absence of any mediators, *Synechocystis*-loaded IO-ITO electrodes gave rise to steady photocurrents with zero decay rate over time, consistent with previous reports.⁸

Since the cytotoxicity assays showed that 200 μ M DCBQ was non-toxic for 72 h (Fig. 3A), the significant decline in the photocurrent output over 15 h could also be attributed to cellular sequestration of the DCBQ molecules over time, which has been shown to occur in *Chlamydomonas reinhardtii*,⁵⁴ or molecular breakdown. To test this, the electrolyte of the photoelectrochemical cell was replaced with fresh BG11 medium alone after 15 h of illumination in the presence of DCBQ, and the photocurrent output was re-measured. The photocurrent densities observed were the same in magnitude as those of *Synechocystis* without DCBQ addition (Fig. 4F). This indicates that cells treated with 200 μ M DCBQ are still viable and photoactive after prolonged exposure, consistent with the cytotoxicity results. Fresh DCBQ was further added to the same set-up and measurements of the photocurrents were taken. In the second DCBQ exposure, the initial mediated photocurrent produced by the *Synechocystis* was 10-fold that of a non-mediated system but was 6-fold lower than that observed during the first DCBQ exposure. The mediated photocurrent (with fresh mediator) eventually returned to the same current density as observed after the first 15 hours. The partial recovery of the mediation effect is consistent with the breakdown or cellular sequestration of DCBQ over time, but the lack of full



recovery points to *Synechocystis* becoming resistant to the mediating effects of DCBQ over time.

The analogous experiment was performed for *Synechocystis* exposed to 200 μ M PYO and light for 15 h (Fig. 4E). In this case, the replacement of electrolyte with fresh BG11 medium gave rise to photocurrent densities that were 4-fold lower than those observed from cells without any exposure to mediators. This indicates that the cells have lost viability from the prolonged exposure to 200 μ M PYO, consistent with the cytotoxicity assays (Fig. 3B). The subsequent addition of fresh PYO to the pre-exposed cells resulted in a 4-fold enhancement in the photocurrents, which implies that the decline in mediated photocurrent output over time was also partially due to a decrease in PYO concentration over time. This may be caused by the cellular sequestration of the mediator, which has been shown to occur for quinones in *Chlamydomonas reinhardtii*,⁵⁴ or to molecular breakdown.

To probe the molecular stability of the PYO and DCBQ, solutions of PYO and DCBQ under light illumination in the presence and absence of redox cycling were studied using cyclic voltammetry and UV-visible spectroscopy (Fig. S10 and S11†). CVs recorded after 15 hours of redox cycling under light illumination for both PYO and DCBQ under atmospheric conditions showed that the redox peaks had almost completely disappeared, indicating that they had both broken down (Fig. S10†) under mediation conditions. UV-vis spectra of PYO before and after 15 hours of light illumination (with no redox cycling) showed no significant differences, indicating PYO is stable under light illumination alone (Fig. S11A†), and the molecular breakdown was likely due to deleterious ROS interactions. UV-vis spectra of DCBQ after 15 hours illumination were significantly changed compared to the spectra recorded before the illumination (Fig. S11B†), and a colour change in the DCBQ solution was observed (Fig. S11C†). Combined, these studies show that DCBQ is intrinsically less chemically stable than PYO.

It can be summarized that both mediators break down over 15 hours, and the mechanism responsible for mediated photocurrent decline over time is different. *Synechocystis* does not become resistant to the mediation effects of PYO over time, though it cannot cope with the excess ROS generated as side products.

Endogenous production of PYO by *Synechocystis*

If the photosynthetic microorganism were able to (re)generate its own mediators endogenously, this would eliminate the need to replenish the microbial devices constantly with synthetic mediators that are lost due to molecular breakdown. Biological production of phenazines in nature is limited to a few bacterial clades, typically occupying soil-dwelling or plant-associated niches, though phenazines are also implicated in human pathogenicity as part of opportunistic *Pseudomonas aeruginosa* infections.⁵⁵ No photosynthetic microorganisms naturally produce phenazines, but two approaches for the endogenous expression of PYO in a microbial photoelectrochemical system are possible; co-culturing cyanobacteria with a PYO producing

bacterial strain, or using genetic engineering to introduce the PYO synthesis pathway to cyanobacteria. As heterologous expression of phenazines has previously been achieved in *E. coli*^{23,24} we attempted to express PYO as an endogenous electron mediator in *Synechocystis*.

Expressing PYO as an endogenous mediator in cyanobacteria is challenging due to the large number of genes required. Biosynthesis of PYO is well characterized, proceeding *via* PCA, which is itself synthesized from the central metabolite chorismate by the seven-gene *phzA-G* operon.²³ Two accessory genes, *phzS* and *phzM* are then required for conversion of PCA to PYO. We built genetic constructs to express the genes as two transcriptional units, one containing the core *phzA-G* genes and the other the accessory *phzSM* genes, from constitutive promoters known to function in *Synechocystis*⁵⁶ (Fig. S12†). Successful expression of the cloned PYO biosynthesis genes from the standard pSB3K3 plasmid was first confirmed in *E. coli*. The production and export of PYO from *E. coli* TOP10 with pSB3K3-PYO was confirmed by UV-visible spectroscopy and mass spectrometry of spent medium from culture grown for four days (Fig. S13†), without any PCA intermediate detected, indicating full conversion.

We initially hypothesized that a PYO producing pathway could be engineered into a previously engineered triple respiratory terminal oxidase (RTO) knockout strain of *Synechocystis* to enhance photocurrent outputs further. The RTO knockout strain lacks the electron sinks cytochrome *c* oxidase, *bd*-quinol oxidase, and the alternative respiratory terminal oxidase, and exhibits power output four-fold higher than the wild-type with ferricyanide as the mediator.⁵⁷ Unexpectedly, in initial screening experiments where PYO was added to an electrode loaded with the RTO knockout mutant, photocurrent diminishment was observed instead of the enhancement seen with wild type cells (Fig. S14†). This can be rationalized by the presence of a higher cellular O_2 concentration in the RTO knockout mutants as a result of the absence of the terminal oxidases, which serves to reduce O_2 back to water. This is consistent with PYO mediation being affected by cellular O_2 levels. Bioengineering efforts therefore focused on introducing the PYO biosynthetic pathway into wild-type *Synechocystis*.

Wild-type *Synechocystis* was transformed with the PYO biosynthesis genes on a broad host range vector backbone (pDF-PYO), and the production and export of PYO was confirmed by mass spectrometry of spent medium from early stationary phase cultures at an OD_{750} of *ca.* 1 (Fig. S15†). The intermediate PCA was not detected in the spent medium using mass spectrometry. The mass for PYO was detected only in the spent medium from *Synechocystis* transformed with pDF-PYO, and not in the negative control strain, which had been transformed with an empty plasmid (pDF-lac), confirming the phenazine is not naturally produced by this cyanobacterium.

The amount of PYO produced and exported by *Synechocystis* with pDF-PYO was measured using UV-visible spectroscopy. A concentration calibration curve using the absorbance of PYO at 690 nm in BG11 medium was plotted and an extinction coefficient of $1.52 \text{ mM}^{-1} \text{ cm}^{-1}$ calculated (Fig. S16†). The concentration of PYO present in the spent medium of early stationary



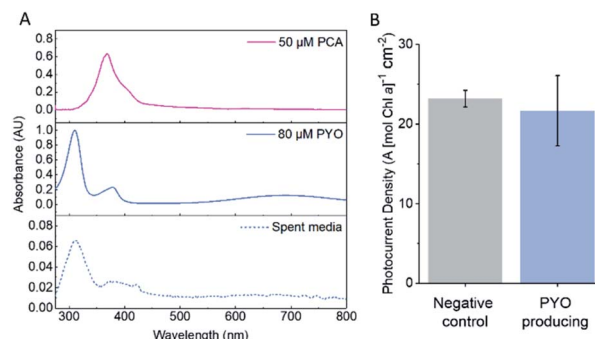


Fig. 5 PYO can be endogenously expressed in *Synechocystis*. (A) A representative UV-vis spectrum of spent medium from continuous cultures of *Synechocystis* transformed with pDF-PYO. Spent medium was taken from mid-late stationary phase cells with an OD₇₅₀ of ca. 1. The spectrum was recorded from 280 to 800 nm with spent medium from the negative control strain taken as the background. UV-vis spectra of PCA (50 µM) and PYO (80 µM) in BG11 medium, with BG11 taken as the backgrounds, are shown for comparison. (B) Photocurrent densities of the negative control *Synechocystis* strain and the PYO producing *Synechocystis* strain with the spent medium in which they were cultured as the electrolyte. All chronoamperometry measurements were recorded at an applied potential of 0.3 V vs. SHE under atmospheric conditions at 25 °C. Light conditions used: 1 mW cm⁻² (50 µE m⁻² s⁻¹) of 680 nm wavelength. Data was collected from 3 biological replicates and the error bars represent SEM ($n = 3$).

phase culture of *Synechocystis* with pDF-PYO was calculated to be 8.2 µM (average of 3 biological replicates) (Fig. 5A), whilst PCA was not detected. However, the concentrations of the phenazines inside of the cells may be significantly higher.

The transformed cells were grown until the culture had reached OD₇₅₀ = 1, concentrated, dropcast on to the porous ITO electrodes and allowed to adhere for 16 hours. The spent BG11 medium from the cultures was retained and used as the electrolyte in the chronoamperometry experiments. There was no significant difference between the photocurrents produced by the negative control strain and the PYO-producing strain (Fig. 5B), which indicates that the concentration of PYO produced is too low for current enhancement.

Optimization of the bioengineering strategy is still needed to increase the production level to match the concentrations needed to enhance photocurrents. This may be achieved by codon optimization of the open reading frames and RBS sequences⁵⁸ and selection of appropriate promoters to increase expression levels of the biosynthesis gene.

Conclusions

In this study, we revealed that energetic gains in cyanobacterial anodes can be achieved using low-potential phenazine mediators, but mediator selection must be based on several criteria. An ideal diffusional electron mediator should: (i) be cell membrane permeable; (ii) be able to mediate electron transfer at concentrations that do not cause cytotoxicity; (iii) participate in minimal deleterious side reactions (for example with O₂); (iv) be robust against deactivation mechanisms such as molecule breakdown to minimize the need for regular replenishments

(noting that endogenous production mitigates this need) and; (v) possess an appropriate midpoint potential to minimize energy loss. This study showed that a fine balance exists between point (v) and the other criteria. The more negative the mid-point potential of the mediator is (and less energy loss from the PETC), the more likely undesirable side reactions with O₂ will occur in addition to kinetics losses. Interestingly, an unexpected example of a deactivation mechanism (point iv) was observed, whereby cells acquired resistance to DCBQ mediation effect over time, which was not observed for PYO.

Although phenazines have only partially fulfilled the aforementioned selection criteria, we show that they exhibit many advantages, including the ability to be endogenously produced by genetically modified cyanobacteria; this is likely to be needed to build low cost microbial photoelectrochemical systems with long lifetimes. Strategies to improve their efficacy could involve, for example, chemical alterations to shift their E_m to slightly higher potentials to avoid oxygen reduction. Synthetic biology approaches could help overcome some of the limitations observed. Strategies for increased phenazine production have been mentioned, but temporal control, for example through coordination with the circadian clock,⁵⁹ could circumvent the issues with oxygen reactivity: phenazines could be released during the night to transfer reducing equivalents that have been generated during the day and stored in reserves of fixed carbon. Expression of enzymes to neutralise ROS (e.g. superoxide dismutase) might decrease the cytotoxicity of phenazines to *Synechocystis*, allowing higher concentrations to be produced. There are many derivatives of biologically produced phenazine, some of which may satisfy more of the criteria listed above, and synthetic biology can be used to expand the variety of phenazine molecules even further.⁶⁰

Establishing long-term efficient wiring of biological systems to electrodes will be key to the success of bio-electrochemical technologies. This study starts to systematically unpick ways of achieving this using diffusional mediators.

Experimental section

Materials

Phenazine (PHZ), 1-hydroxyphenazine (1-OHP), pyocyanin (PYO), 2,5-dichloro-1,4-benzoquinone (DCBQ), phenazine-1-carboxylic acid (PCA), 3-(3,4-dichlorophenyl)-1,1-dimethylurea (DCMU) and methyl viologen (MV) used in this study were commercially sourced and used without further purification.

Biological samples

Escherichia coli TOP10 was used for cloning and expression of phenazine genes. All *E. coli* strains were cultured at 37 °C and with 200 rpm shaking in LB-Lennox medium supplemented with antibiotics where appropriate. Replicative plasmids were transformed into *Synechocystis* by tri-parental mating. Wild-type, triple RTO knockout and plasmid-bearing derivatives of *Synechocystis* sp. PCC 6803 (GT-I) were cultured photoautotrophically under 1 mW cm⁻² (50 µE m⁻² s⁻¹) continuous white light at 30 °C in BG11 medium, supplemented with

spectinomycin where appropriate. Spent medium from cultures was obtained by centrifugation at 5000g for 10 min and microfiltration of the supernatant (pore size = 0.2 μm , Whatman®).

Cloning

The *phzA-G* operon encoding the genes required for PCA biosynthesis, including the native RBS sequences, was cloned from *P. aeruginosa* PAO1. The *phzS* and *phzM* genes required for PYO production were obtained through a combination of DNA synthesis and lab-based DNA assembly and were combined along with their native RBS sequences into a synthetic bicistronic operon. Further details of the cloning strategy, plus a list of plasmids and BioBrick parts can be found in ESI.† Plasmids pUC19-*phzAG* and pSB3C5-*phzM* carrying the phenazine bio-production operon BioBricks have been submitted to the Addgene repository (plasmids #141105 and #141106).

Calculated log D determination

These were performed in ChemAxon Marvin using the LogD plugin.⁶¹ LogD values were calculated to 3 decimal places between pH 4–10 for all mediators used in this study.

Toxicity assays

Wild-type *Synechocystis* cells (5 nmol Chl *a*) were incubated with different concentrations of PCA, PYO and DCBQ for 1 or 3 days, as stated, under conditions described above. *Synechocystis* cells incubated in BG11 with no electron mediator or in BG11 with 0.2% (v/v) DMSO solvent under the same conditions were used as controls. Following incubation, the cells were resuspended in fresh BG11 and their concentration standardized to an optical density at 750 nm (OD₇₅₀) of 0.5. Aliquots (10 μL) of three serial dilutions ($\times 1$, $\times 10^{-3}$, $\times 10^{-6}$) were spotted on BG11 agar and the plates incubated for 1 week at 30 °C under 1 mW cm⁻² (50 $\mu\text{E m}^{-2} \text{s}^{-1}$) white light. The growth of the cells pre-incubated with mediator was compared to the controls by eye to assess the cytotoxicity of the mediators.

Detection of PCA and PYO in spent medium

To detect PYO production from *E. coli* and *Synechocystis*, UV-visible spectroscopy (Varian Cary 50 Bio UV-vis spectrometer) was performed between 200 and 800 nm on the spent medium from the plasmid-bearing derivatives of *E. coli* and *Synechocystis*. *E. coli* was grown from mid-log phase for a further 4 days before taking the spent medium; *Synechocystis* was grown from mid-log phase to early stationary phase at an OD₇₅₀ of *ca.* 1 before taking the spent medium. Spectra of solid PYO dissolved in LB medium (125 μM) and BG11 medium (80 μM) were also obtained to help validate the results. Mass spectrometry (MS) was performed using a Waters Vion IMS Qtof Mass Spectrometer on spent medium from the negative control strains and the PYO producing strains of *E. coli* and *Synechocystis* to detect the presence of PYO.

Synechocystis-electrode preparation

Inverse opal mesoporous ITO (IO-ITO) electrodes with 10 μm pore size were prepared using the method reported in Zhang *et al.*⁸ Planktonic cultures of early stationary phase *Synechocystis* at an OD₇₅₀ of *ca.* 1 were concentrated by centrifugation at 5000g for 10 min, the supernatant removed and the pellet resuspended in fresh BG11 medium to a concentration of 150 nmol Chl *a* mL⁻¹. 250 μL of this was dropcast onto the IO-ITO electrodes and left overnight at room temperature in a covered humid chamber in the dark to allow cell adhesion, yielding *Synechocystis*-loaded electrodes the following day which were used immediately for analysis.

(Photo)electrochemical measurements

All (photo)electrochemical measurements were performed at 25 °C using an Ivium Technologies CompactStat, an Ag/AgCl (saturated) reference electrode (corrected by +0.197 V for SHE), a platinum mesh counter electrode and a glassy carbon (diameter = 3 mm) or a IO-ITO working electrode. Experiments were carried out with light/dark cycles, using a collimated LED light source (1 mW cm⁻² (50 $\mu\text{E m}^{-2} \text{s}^{-1}$), 680 nm, Thorlabs). All (photo)electrochemical measurements were performed in BG11 electrolyte at pH 8.5 unless otherwise stated.

Cyclic voltammetry measurements were recorded in BG11 electrolyte at 25 °C with a glassy carbon or ITO working electrode. Unless stated otherwise, the electrolyte was bubbled with N₂ gas for 20 min to purge the system of O₂, and a stream of N₂ was maintained in the headspace during the experiment.

Chronoamperometry experiments were performed with a dark/light cycle of two minutes off, two minutes on. In the longevity study a dark/light cycle of 3 min off, 1 hour on was used. Photocurrents were normalised against the geometric area of the electrode (0.75 cm² for IO-ITO electrodes).

The Chl *a* content of the *Synechocystis*-loaded electrode was determined by scraping off the annealed ITO nanoparticles from the FTO coated glass into methanol, sonicating the suspension for 15 min in iced water, then centrifuging at 12 000g for 2 min. The supernatant was analysed by UV-vis spectroscopy and the Chl *a* concentration was determined using the extinction co-efficient of Chl *a* at 665.5 nm in methanol (70 020 [mol Chl *a*]⁻¹ dm³ cm⁻¹).⁶² Photocurrents were background corrected by subtracting the dark current from the chronoamperometry profile.

In the longevity studies, the total charge delivered by the *Synechocystis*-loaded electrodes during each light cycle was found by integrating the background corrected photocurrents. From this, the turn-over number (TON) and turn-over frequency (TOF) were calculated using the method described by Zhang *et al.*⁸ TONs from consecutive light cycles were summed to find the cumulative TON.

Author contributions

EC performed most of the electrochemistry experiments, RB performed all synthetic biology experiments, LTW and JML contributed to cell culturing and electrochemical experiments,

XC prepared the electrodes. EC, RB and JZ wrote the manuscript, and all authors contributed to discussions and interpretations of the results. All authors have given approval to the final version of the manuscript.

Abbreviations

BG11 medium	Blue green-11 medium
BPVs	Biophotovoltaics
DCBQ	2,6-Dichloro-1,4-benzoquinone
DCMU	3-(3,4-Dichlorophenyl)-1,1-dimethylurea
EET	Extracellular electron transfer
1-OHP	1-Hydroxyphenazine
MV	Methyl viologen
MFCs	Microbial fuel cells
PHZ	Phenazine
PCA	Phenazine-1-carboxylic acid
PETC	Photosynthetic electron transport chain
PSI	Photosystem I
PSII	Photosystem II
Q_A and Q_B	Plastoquinones
PYO	Pyocyanin
RBS	Ribosome binding site
ROS	Reactive oxygen species
SHE	Standard hydrogen electrode
TOF	Turn-over frequency
TON	Turn-over number

Conflicts of interest

There are no conflicts to declare.

Acknowledgements

This work was supported by the Cambridge Trust (LTW) and the Biotechnology and Biological Sciences Research Council (BB/M011194/1 to JML, BB/R009171/1 and BB/K016288/1 to RB, BB/R011923/1 to JZ, EC and XC). We thank Prof. Nicolas Plumeré for his feedback on this manuscript and Dr Paolo Bombelli for helpful discussions.

References

- 1 R. W. Bradley, P. Bombelli, S. J. L. Rowden and C. J. Howe, *Biochem. Soc. Trans.*, 2012, **40**, 1302–1307.
- 2 K. L. Saar, P. Bombelli, D. J. Lea-Smith, T. Call, E.-M. Aro, T. Müller, C. J. Howe and T. P. J. Knowles, *Nat. Energy*, 2018, **3**, 75–81.
- 3 M. Sawa, A. Fantuzzi, P. Bombelli, C. J. Howe, K. Hellgardt and P. J. Nixon, *Nat. Commun.*, 2017, **8**, 1–10.
- 4 J. Tschorntner, B. Lai and J. O. Krömer, *Front. Microbiol.*, 2019, **10**, 866.
- 5 J. Z. Zhang and E. Reisner, *Nat. Rev. Chem.*, 2020, **4**, 6–21.
- 6 A. J. McCormick, P. Bombelli, R. W. Bradley, R. Thorne, T. Wenzel and C. J. Howe, *Energy Environ. Sci.*, 2015, **8**, 1092–1109.
- 7 J. Barber and P. D. Tran, *J. R. Soc., Interface*, 2013, **10**, 20120984.
- 8 J. Z. Zhang, P. Bombelli, K. P. Sokol, A. Fantuzzi, A. W. Rutherford, C. J. Howe and E. Reisner, *J. Am. Chem. Soc.*, 2018, **140**, 6–9.
- 9 N. Kornienko, J. Z. Zhang, K. K. Sakimoto, P. Yang and E. Reisner, *Nat. Nanotechnol.*, 2018, **13**, 890–899.
- 10 G. Longatte, A. Sayegh, J. Delacotte, F. Rappaport, F.-A. Wollman, M. Guille-Collignon and F. Lemaître, *Chem. Sci.*, 2018, **9**, 8271–8281.
- 11 R. M. Schuurmans, J. M. Schuurmans, M. Bekker, J. C. Kromkamp, H. C. P. Matthijs and K. J. Hellingwerf, *Plant Physiol.*, 2014, **165**, 463–475.
- 12 L. T. Wey, P. Bombelli, X. Chen, J. M. Lawrence, C. M. Rabideau, S. J. L. Rowden, J. Z. Zhang and C. J. Howe, *ChemElectroChem*, 2019, **6**, 5375–5386.
- 13 A. Cereda, A. Hitchcock, M. D. Symes, L. Cronin, T. S. Bibby and A. K. Jones, *PLoS One*, 2014, **9**, e91484.
- 14 P. Bombelli, R. W. Bradley, A. M. Scott, A. J. Philips, A. J. McCormick, S. M. Cruz, A. Anderson, K. Yunus, D. S. Bendall, P. J. Cameron, J. M. Davies, A. G. Smith, C. J. Howe and A. C. Fisher, *Energy Environ. Sci.*, 2011, **4**, 4690.
- 15 S. D. Minteer, B. Y. Liaw and M. J. Cooney, *Curr. Opin. Biotechnol.*, 2007, **18**, 228–234.
- 16 J. Barber and M. D. Archer, *J. Photochem. Photobiol. A*, 2001, **142**, 97–106.
- 17 Y. Kato, R. Nagao and T. Noguchi, *Proc. Natl. Acad. Sci. U. S. A.*, 2016, **113**, 620–625.
- 18 K. Brettle, *Biochim. Biophys. Acta, Bioenerg.*, 1997, **1318**, 322–373.
- 19 R. D. Finn, J. Basran, O. Roitel, C. R. Wolf, A. W. Munro, M. J. I. Paine and N. S. Scrutton, *Eur. J. Biochem.*, 2003, **270**, 1164–1175.
- 20 A. Price-Whelan, L. E. P. Dietrich and D. K. Newman, *J. Bacteriol.*, 2007, **189**, 6372–6381.
- 21 A. Price-Whelan, L. E. P. Dietrich and D. K. Newman, *Nat. Chem. Biol.*, 2006, **2**, 71–78.
- 22 L. S. Pierson and E. A. Pierson, *Appl. Microbiol. Biotechnol.*, 2010, **86**, 1659–1670.
- 23 D. V. Mavrodi, R. F. Bonsall, S. M. Delaney, M. J. Soule, G. Phillips and L. S. Thomashow, *J. Bacteriol.*, 2001, **183**, 6454–6465.
- 24 J. Feng, Y. Qian, Z. Wang, X. Wang, S. Xu, K. Chen and P. Ouyang, *J. Bacteriol.*, 2018, **275**, 1–6.
- 25 K. Rabaey, N. Boon, S. D. Siciliano, M. Verhaeghe and W. Verstraete, *Appl. Environ. Microbiol.*, 2004, **70**, 5373–5382.
- 26 K. Rabaey, N. Boon, M. Höfte and W. Verstraete, *Environ. Sci. Technol.*, 2005, **39**, 3401–3408.
- 27 T. Zhang, L. Zhang, W. Su, P. Gao, D. Li, X. He and Y. Zhang, *Bioresour. Technol.*, 2011, **102**, 7099–7102.
- 28 T. H. Pham, N. Boon, K. De Maeyer, M. Höfte, K. Rabaey and W. Verstraete, *Appl. Microbiol. Biotechnol.*, 2008, **80**, 985–993.
- 29 J. Z. Zhang, K. P. Sokol, N. Paul, E. Romero, R. van Grondelle and E. Reisner, *Nat. Chem. Biol.*, 2016, **12**, 1046–1052.
- 30 S. G. Hays, L. L. Yan, P. A. Silver and D. C. Ducat, *J. Biol. Eng.*, 2017, **11**, 4.



31 Y. Wang and D. K. Newman, *Environ. Sci. Technol.*, 2008, **42**, 2380–2386.

32 G. Inzelt and Z. Puskás, *Electrochim. Acta*, 2004, **49**, 1969–1980.

33 D. Mersch, C.-Y. Lee, J. Z. Zhang, K. Brinkert, J. C. Fontecilla-Camps, A. W. Rutherford and E. Reisner, *J. Am. Chem. Soc.*, 2015, **137**, 8541–8549.

34 Y. Umena, K. Kawakami, J.-R. Shen and N. Kamiya, *Nature*, 2011, **473**, 55–60.

35 P. Jordan, P. Fromme, H. T. Witt, O. Klukas, W. Saenger and N. Krauß, *Nature*, 2001, **411**, 9.

36 M. Grattieri, Z. Rhodes, D. P. Hickey, K. Beaver and S. D. Minteer, *ACS Catal.*, 2019, **9**, 867–873.

37 N. Kornienko, J. Z. Zhang, K. P. Sokol, S. Lamaison, A. Fantuzzi, R. van Grondelle, A. W. Rutherford and E. Reisner, *J. Am. Chem. Soc.*, 2018, **140**, 17923–17931.

38 M. J. Waring, *Bioorg. Med. Chem. Lett.*, 2009, **19**, 2844–2851.

39 T. Yagishita, S. Sawayama, K. Tsukahara and T. Ogi, *Sol. Energy*, 1997, **61**, 347–353.

40 G. Longatte, F. Rappaport, F.-A. Wollman, M. Guille-Collignon and F. Lemaître, *Electrochim. Acta*, 2017, **236**, 337–342.

41 N. Sekar, Y. Umasankar and R. P. Ramasamy, *Phys. Chem. Chem. Phys.*, 2014, **16**, 7862–7871.

42 L. Beauzamy, J. Delacotte, B. Bailleul, K. Tanaka, S. Nakanishi, F.-A. Wollman and F. Lemaître, *Anal. Chem.*, 2020, **92**, 7532–7539.

43 L. E. P. Dietrich, A. Price-Whelan, A. Petersen, M. Whiteley and D. K. Newman, *Mol. Microbiol.*, 2006, **61**, 1308–1321.

44 C. D. Cox, *Infect. Immun.*, 1986, **52**, 8.

45 D. J. Hassett, L. Charniga, K. Bean, D. E. Ohman and M. S. Cohen, *Infect. Immun.*, 1992, **60**, 328–336.

46 K. J. Reszka, Y. O’Malley, M. L. McCormick, G. M. Denning and B. E. Britigan, *Free Radicals Biol. Med.*, 2004, **36**, 1448–1459.

47 S. S. Baron, G. Terranova and J. J. Rowe, *Curr. Microbiol.*, 1989, **18**, 223–230.

48 V. Proux-Delrouyre, C. Demaille, W. Leibl, P. Sétif, H. Bottin and C. Bourdillon, *J. Am. Chem. Soc.*, 2003, **125**, 13686–13692.

49 C. L. Bird and A. T. Kuhn, *Chem. Soc. Rev.*, 1981, **10**, 49–82.

50 O. Simoska, M. Sans, L. S. Eberlin, J. B. Shear and K. J. Stevenson, *Biosens. Bioelectron.*, 2019, **142**, 111538.

51 N. R. Glasser, B. X. Wang, J. A. Hoy and D. K. Newman, *J. Biol. Chem.*, 2017, **292**, 5593–5607.

52 K. K. Karukstis, S. C. Boegeman, J. A. Fruetel, S. M. Gruber and M. H. Terris, *Biochim. Biophys. Acta, Bioenerg.*, 1987, **891**, 256–264.

53 K. K. Karukstis, S. M. Gruber, J. A. Fruetel and S. C. Boegeman, *Biochim. Biophys. Acta, Bioenerg.*, 1988, **932**, 84–90.

54 G. Longatte, H.-Y. Fu, O. Buriez, E. Labbé, F.-A. Wollman, C. Amatore, F. Rappaport, M. Guille-Collignon and F. Lemaître, *Biophys. Chem.*, 2015, **205**, 1–8.

55 D. V. Mavrodi, T. L. Peever, O. V. Mavrodi, J. A. Parejko, J. M. Raaijmakers, P. Lemanceau, S. Mazurier, L. Heide, W. Blankenfeldt, D. M. Weller and L. S. Thomashow, *Appl. Environ. Microbiol.*, 2010, **76**, 866–879.

56 E. Englund, F. Liang and P. Lindberg, *Sci. Rep.*, 2016, **6**, 36640.

57 R. W. Bradley, P. Bombelli, D. J. Lea-Smith and C. J. Howe, *Phys. Chem. Chem. Phys.*, 2013, **15**, 13611.

58 K. Thiel, E. Mulaku, H. Dandapani, C. Nagy, E.-M. Aro and P. Kallio, *Microb. Cell Fact.*, 2018, **17**, 34.

59 K. Kucho, K. Okamoto, Y. Tsuchiya, S. Nomura, M. Nango, M. Kanehisa and M. Ishiura, *J. Bacteriol.*, 2005, **187**, 2190–2199.

60 S. Guo, R. Liu, W. Wang, H. Hu, Z. Li and X. Zhang, *ACS Synth. Biol.*, 2020, **9**, 883–892.

61 Calculator Plugins were used for structure property prediction and calculation, *Marvin 20.12.0*, 2020, ChemAxon, <http://www.chemaxon.com>.

62 Y. Li, N. Scales, R. E. Blankenship, R. D. Willows and M. Chen, *Biochim. Biophys. Acta, Bioenerg.*, 2012, **1817**, 1292–1298.

